Case Studies in Thermal Engineering 51 (2023) 103552

Contents lists available at ScienceDirect

Case Studies in Thermal Engineering

journal homepage: www.elsevier.com/locate/csite

Implication of radiation on the thermal behavior of a partially wetted dovetail fin using an artificial neural network

P. Nimmy [a], K.V. Nagaraja [a], Pudhari Srilatha [b], K. Karthik [c], G. Sowmya [d], R.S. Varun Kumar [a], Umair Khan [e,f,g], Syed Modassir Hussain [h,*], A.S. Hendy [i], Mohamed R. Ali [j,k]

[a] Department of Mathematics, Amrita School of Engineering, Amrita Vishwa Vidyapeetham, Bengaluru, 560035, India
[b] Department of Mathematics, Institute of Aeronautical Engineering, Hyderabad, 500043, India
[c] Department of Studies and Research in Mathematics, Davangere University, Davangere, 577002, Karnataka, India
[d] Department of Mathematics, M S Ramaiah Institute of Technology, Bangalore, 560054, Karnataka, India
[e] Department of Mathematical Sciences, Faculty of Science and Technology, University Kebangsaan Malaysia, UKM, Bangi, 43600, Selangor, Malaysia
[f] Department of Mathematics and Social Sciences, Sukkur IBA University, Sukkur 65200, Sindh, Pakistan
[g] Department of Computer Science and Mathematics, Lebanese American University, Byblos, Lebanon
[h] Department of Mathematics, Faculty of Science, Islamic University of Madinah, Madinah, 42351, Saudi Arabia
[i] Department of Computational Mathematics and Computer Science, Institute of Natural Sciences and Mathematics, Ural Federal University, 19 Mira St., 620002, Yekaterinburg, Russia
[j] Faculty of Engineering and Technology, Future University in Egypt, New Cairo, 11835, Egypt
[k] Basic Engineering Science Department, Benha Faculty of Engineering, Benha University, Benha, Egypt

ARTICLE INFO

Handling Editor: Huihe Qiu

Keywords:
Fin
Dovetail fin
Partially wet fin
Artificial neural network

ABSTRACT

The simultaneous convection-radiation heat transfer of a partially wetted dovetail extended surface is investigated in this study. Also, the temperature variance behavior of the dovetail extended surface (DES) is estimated through thermal models for partially wet and dry conditions using the neural network with the Levenberg-Marquardt scheme (NNLMS). The corresponding governing energy equations of a dovetail fin are presented as a set of ordinary differential equations (ODE), which are reduced to a non-dimensional form using dimensionless terms. Further, the resulting coupled conductive, convective, and radiative dimensionless ODEs are numerically solved utilizing the Runge-Kutta-Fehlberg fourth-fifth order (RKF-45) scheme. Using graphical illustrations, the resultant solutions are physically determined by considering the effects of various nondimensional variables on thermal behavior. From the outcomes, it is established that the thermal conductivity parameter enhances the thermal distribution in a partially wetted dovetail fin, and an upsurge in convection-conduction variable, temperature ratio parameter, radiation-conduction, and wet parameter diminishes the temperature profile of the considered extended surface. The modelled problem's NNLMS efficacy is demonstrated by achieving the best convergence and unique numerically assessed quantified results. The outcomes indicate that the strategy successfully resolves the partially wetted fin problem.

* Corresponding author.
E-mail addresses: nimmyvanamohan@gmail.com (P. Nimmy), kv_nagaraja@blr.amrita.edu (K.V. Nagaraja), pudhari.srilatha@gmail.com (P. Srilatha), karthik.dumaths@gmail.com (K. Karthik), g.sowmya34@gmail.com (G. Sowmya), rs_varun@blr.amrita.edu (R.S.V. Kumar), umairkhan@iba-suk.edu.pk (U. Khan), hussain.modassir@yahoo.com (S.M. Hussain), Ahmed.hendy@fsc.bu.edu.eg (A.S. Hendy), mohamed.reda@fue.edu.eg (M.R. Ali).

https://doi.org/10.1016/j.csite.2023.103552
Received 6 July 2023; Received in revised form 16 September 2023; Accepted 27 September 2023
Available online 4 October 2023

Nomenclature:

P	Perimeter of the fin $[m]$
C	Fin taper ratio
L_d	Dimensionless wet length
T	Temperature $[m]$
$t(\xi)$	Fin's semi-thickness $[m]$
$k^*(T)$	Thermal conductivity $[W/(mK)]$
κ	Thermal conductivity variation parameter
Nt	Temperature ratio parameter
X	Length of the fin (dimensionless)
W	Width $[m]$
T_a	Ambient temperature $[K]$
c_p	Specific heat $[J/(kgK)]$
h^*	Convective heat transfer coefficient $[W/(m^2K)]$
Le	Lewis number
ω	humidity ratio
β	Thermal conductivity coefficient (dimensionless)
b_2	Variable parameter $[/K]$
Nr	Radiation-conduction parameter
ψ	Wet parameter
Θ	Non-dimensional temperature
ξ	Fin axial distance $[m]$
t_b	Thickness $[m]$
L	Length $[m]$
σ	Stefan-Boltzmann constant $[W/(m^2K^4)]$
ε^*	Emissivity
h_D	Mass transfer convective coefficient $[kg/(m^2s)]$
Nc	Convection-conduction variable
i_{fg}	Latent heat of evaporation $[J/kg]$
ω_a	Specific humidity

1. Introduction

Heat release during a thermal process is becoming indispensable in various engineering applications, including radiators, gas turbines, automobiles, microprocessors, and air conditioners. For the substantial development in recent technology, enhancing heat transfer or heat dissipation process for attaining a greater heat transmission rate has turned out to be one of the chief issues. Optimizing heat transmission in heating and cooling systems has been emphasized as a key approach that will enhance their performance, and it is possible to achieve this by utilizing the heat transfer fluid with nanofluid. The nanofluid has been the subject of study by numerous researchers due to its industrial significance in heat transfer processes [1–9]. However, there has been a generous need for lightweight, efficient, cost-effective equipment for managing heat dispersal rates in recent years. The excess heat will be a prodigious threat to electrical and electronic gadgets. Thus, safety measures must be taken to sustain the system's performance by dispelling the generated heat into the atmosphere. Typically, an upsurge in temperature difference, heat transfer coefficient (HTC), and heat exchanging area will amplify the heat transmission rate. Since the temperature difference is restricted by technology, it cannot be amplified much, and enhancing the HTC is a challenge nowadays. Thus, extending the heat transferring area is considered as one of the most appropriate solutions for increasing the heat exchange. This extending surface area is recognized as a fin (extended surface). Fins are thin metal strips anchored for up-surging heat transference between a surface and the neighboring fluid. Fins have potential applications in numerous industrial sectors, including combustion engines, radiators, electrical motors, electronic chips, compressors, transformers, solar collectors, refrigerators, and heat sinks. The core aim of the fin industry is to curtail the dimension and expense of fins. The increased cost of the high-thermal-conductivity metals involved in producing finned surfaces and the cost associated with the weight of the fin frequently served as a justification for this necessity. By enhancing heat transmission from fins, these objectives can be accomplished. Increasing the thermal conductivity, HTC between the surrounding fluid and the surface of the solid fin, and the fin's surface area to volume ratio are all methods that can be used to achieve this increase. Numerous investigators contributed their extensive research works associated with heat transmission through fins. Transient heat transport in fins enduring radiative and convective heat dissipation was deliberated by Ndlovu [10]. Their results illustrated how parameter variations might influence the fin's temperature distribution, and the convective-radiative boundary conditions at the fin tip improve heat transfer via extended surfaces. Sarwe and Kulkarni [11] analyzed heat transference through an annular extended surface having varied thermal conductivity

by employing the differential transform method. The results disclosed that as the varying thermal conductivity variable, the fin's thermal gradient enhances, and larger thermogeometric parametrical values result in greater heat transmission. The efficiency of stretching/shrinking extended surface of a rectangular profile for improving the heat transfer rate was explicated by Din et al. [12]. Their results revealed that the fin's tip temperature escalates with increasing Peclet number. The characteristics of the thermal dispersion of a lateral extended surface were investigated by Gouran et al. [13], and their investigation concluded that with the execution of this type of fin, radiative-conductive impact results in superior cooling performance. The conductive radiative thermal distribution in an annular fin having a rectangular profile was scrutinized by Kumar et al. [14]. Their findings divulged that the highest temperature is at the fin's base, and the lowest is at the fin's tip. Investigations dealing with heat transfer employing various fins have recently been reported [15–18]. As a consequence of the ever-increasing quest for heat-augmenting devices, immense research work has been carried out in the field of various fin designs comprising longitudinal, radial, annular, porous, spine, pin, trapezoidal, and inverted trapezoidal fins. Fins constituting the rectangular profile have been widely used because of their affordable price and ease of manufacture. Parabolically structured fins are preferred over rectangular profiled fins in modeling elements where weight is a factor, such as aviation applications. However, because of its curve-like structure, parabolic fins are more problematic in manufacturing and are expensive. Moreover, the sharp edge of a triangular fin causes safety concerns. Rather than other configured fins, trapezoidal fin produces more generalizable and convenient efficiency. Consequently, a trapezoidal fin is one of the utmost resolutions in terms of lightweight and safety. Apart from using trapezoidal fins, several researchers showed their interest in the usage of inverted or reversed trapezoidal fins. Reversed trapezoidal fins, also called dovetail fins, can convey more thermal energy with an equivalent base area compared to a rectangular profiled extended surface. Also, better heat distribution over a larger area can be achieved using these fins. The design and functioning of the dovetail fin were explained by Lane and Heggs [19]. From their research point of view, it can be concluded that heat flow is greater in dovetail fin compared to tapered fin. Convective-radiative heat transfer through different profiled fins, including dovetail shape was analyzed by Khan et al. [20]. According to the outcomes of their investigation, it has been revealed that followed by fins having trapezoidal and rectangular profiles, the one with a dovetail design resulted in a superior heat transmission rate. Gamaoun et al. [21] scrutinized thermal distribution in a dovetail fin by utilizing the Cattaneo-Vernotte model. They concluded that dovetail fins have a higher temperature profile than rectangular profiled fins.

Typically, in air conditioning systems, the surface temperature of cooling coils is lower than that of the dew point temperature (DPT) of the air that is being refrigerated. Thus, as an upshot, mass and heat transfer occur concurrently, and the extended surface's overall efficiency is affected by moisture condensation on the fin surface. Depending upon the variance between the surface temperature and the DPT, fin surfaces are classified into three categories: fully dry, partially wet, and fully wet. If the temperature of the outer surface is greater than the DPT of the moist air, then there is only adequate heat transfer between them, and at this stage, the fin is supposed to be in a fully dry condition. Meanwhile, a fully wet condition occurs if the temperature at the tip of the extended surface is significantly lower than that of the DPT of moist air. Consequently, a peculiar scenario occurs when the temperature at the base of the extended surface drops, and the temperature at the fin's tip exceeds the atmospheric air's DPT. This situation resulted in a partially wetted fin. Hence, if the extended surface is partially wet, relative humidity severely influences its efficiency. Research in this field is limited, although some have concentrated on the thermal performance of different profiled fins under partially wet conditions (PWC). The efficiency of a rectangular extended surface under dry, partially, and fully wet conditions was analyzed by Mao et al. [22]. They found that as the aspect ratio of fin length to width decreases, the heat transmission in the dry region increases, particularly for partially wet fin. If the relative humidity becomes greater than 29.08%, the fin surface becomes partially wet. For differently profiled longitudinal fins, the extended surface efficiencies under a partially wet surface were presented by Pirompugd and Wongwises [23]. Their investigations concluded that with an intensification in relative humidity, the fin efficacy under partially humid circumstances was found to be decreased. The thermal performance of a circular extended surface was deliberated by Pashah et al. [24]. Under both fully and PWC, the actual temperature-humidity ratio under entirely and partially wet operational circumstances is considered. The results showed that because of the non-linear actual psychrometric linkage between humidity ratio and temperature of the air, the numerical solution obtained is more appropriate for hyperbolic fins that are partially wet in condition. Hazarika et al. [25] analyzed the optimal design of fork-shaped extended surface functioning at PWC. Their findings revealed that the fin surface become partially wet as the least fin gap or fin volume is enlarged. The efficiency of annular fins under PWC was analytically investigated by Pirompugd and Wongwises [26].

In engineering heat transfer mechanisms, the need for computer-based algorithms is in great demand. Algorithms based on artificial intelligence are the simplest models of human intelligence and evolutionary experience. The techniques involved in the augmentation of heat transfer processes comprise the usage of equations, employing standard correlations, constructing new designs, and, lastly, through the trial-and-error method, experimental data can be gathered. Since heat transfer problems are becoming more complex, while dealing with the dynamics performance of the corresponding system, the necessity for figuring out steady-state phenomena is also growing. To tackle this difficulty, a simple neural network, namely an Artificial neural network (ANN) has been implemented in various heat transfer studies which are merely based on existing data. ANN is a data processing architecture influenced by biologically related neuron systems of the human brain and is assembled by a bulk number of interconnecting elements called neurons. Without having fundamental knowledge about the physical systems, ANNs can simulate the connection between any collection of input and output data. Designing steam-developing plants, forecasting airflows in ventilated rooms, recovering waste heat from heat exchangers, and analyzing the thermal process are merely a few of the heat transference applications in which ANN has been successfully employed. Since ANN responses are speedy and reliable in predicting performances; they are more advantageous in the simulation of thermal processes. Pothina and Nagaraja [27] explained the mathematics behind the construction of artificial neurons by considering the activation functions. Their work helped in the structuring of neural networks which has been implemented by the help of mathematical models. Researchers are now highly captivated to contribute their research wealth in the field of ANN. Naphon et al.

[28] inspected the characteristics of heat transference and jet impingement of nanoliquid in a heat sink by proposing an ANN model. Their two-phase model contributed to a thorough understanding of energy transfer augmentation in microchannel heat sinks. Ahmad et al. [29] probed the temperature dispersal through a permeable extended surface by exploring ANN models. They concluded that compared to other numerical methods; the suggested ANN model had leveled up accuracy and since the fin must transmit a large amount of heat to the surrounding region in steady circumstances, the amplified heat generation maximizes the temperature of the fin. Skrypnik et al. [30] presented an innovative model of ANN for the prediction of HTC and friction factor in tubes having an inner helical filling. By employing this new proposed model of ANN, the friction factor and Nusselt number were generalized, and the outcomes revealed a good agreement among them when compared with the evaluated and experimental data. By implementing ANN methods, Kumar et al. [31] emphasized the heat transfer phenomena along a longitudinal fin. They used ANN to solve the dimensionless problem concerned with the stretch and shrink of the fin. Their results divulged that ANNs have higher correlational and interpretative strength for evaluating heat transfer. Kumar et al. [32] implemented the differential evolution-based ANN to predict the heat transmission characteristics of the permeable wavy fin.

Researchers have conducted significant studies on the thermal performance of fins under partially wet and dry situations. However, the temperature distribution in a dovetail fin under partially wet and partially dry conditions has not yet been investigated. So, the thermal dispersal behavior in the dovetail profiled fin under PWC is discussed with the impact of convective-radiative heat dispersal. The NNLMS is employed to investigate the heat transmission in the extended surface. The model that governs the energy equation of a dovetail fin is expressed as a system of ODEs, which is simplified to a non-dimensional representation using dimensionless variables. Additionally, the RKF-45 methodology is employed to solve the dimensionless ODEs. The consequence of various dimensionless constraints on the thermal profile of the dovetail fin is shown graphically.

2. Modelling of the problem

The steady-state heat transfer and thermal performance of a partially wetted convective dovetail extended surface transferring heat to the adjacent at T_a are considered in this investigation, as demonstrated in Fig. 1. The following presumptions establish the core of the comprehensive analysis:

- The transport of heat by radiation and convection has been taken into account.
- The fin renders no internal heat during the heat transmission.
- Due to the fin's thinness in relation to the remaining measurements, it is assumed that the temperature dispersion is one-dimensional.
- The thermal conductivity of the DES is taken as temperature dependent and adiabatic fin tip is assumed.
- The surface heat transfer coefficient is assumed as a power law function of temperature and the latent heat of condensation of the moisture is assumed to remain constant.

Mathematical representation of the partially wetted fin model driven by mass and energy conservation laws is developed which is specified as (Pirompugd and Wongwises [23] and Kundu [33]):

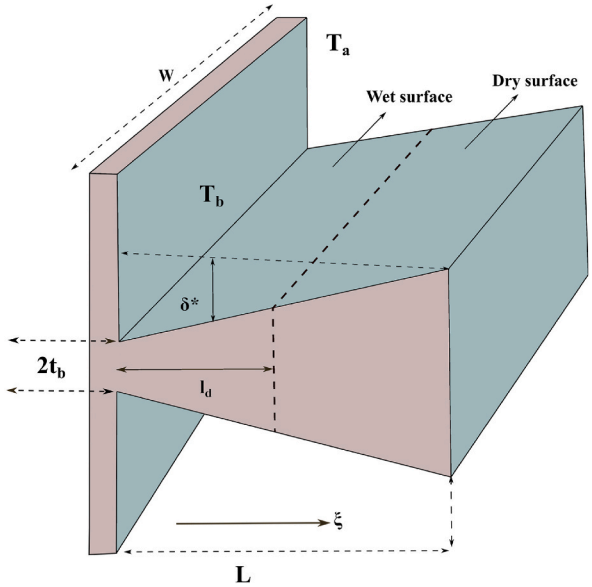

Fig. 1. Graphical depiction of a dovetail fin.

$$\frac{d}{d\xi}\left[k^*(T)t(\xi)\frac{dT}{d\xi}\right] = h^*(T)(T-T_a) + h_D i_{fg}(\omega-\omega_a) + \sigma\,\varepsilon^*\left(T^4-T_a^4\right), 0 \le \xi \le l_d \tag{1}$$

In the above equation, i_{fg} indicates latent heat of condensation, ω_a specifies humidity ratio of the atmospheric air, and ω denotes humidity ratio of saturated air at T. If the overall temperature of the extended surface surpasses than the neighboring air's DPT, the fin region is regarded as dry, and i_{fg} is taken to be zero. For this case, the following equation denotes the balanced energy transfer in the dry region ($l_d \le \xi \le L$) of the DES.

$$\frac{d}{d\xi}\left[k^*(T)t(\xi)\frac{dT}{d\xi}\right] = h^*(T)(T-T_a) + \sigma\,\varepsilon^*\left(T^4-T_a{}^4\right), l_d \le \xi \le L, \tag{2}$$

where, l_d denotes the region separating the dry and wet portions and thickness of DES is given as

$$t(\xi) = t_b - \delta^*\left(\frac{\xi}{L}\right). \tag{3}$$

Substitution of Eq. (3) in Eq. (1) and Eq. (2) yields,

$$\frac{d}{d\xi}\left[k^*(T)\left[t_b-\delta^*\left(\frac{\xi}{L}\right)\right]\frac{dT}{d\xi}\right] = \begin{matrix} h^*(T)(T-T_a) + h_D i_{fg}(\omega-\omega_a) \\ +\sigma\varepsilon^*\left(T^4-T_a^4\right) \end{matrix}, 0 \le \xi \le \mathrm{l_d}, \tag{4}$$

and

$$\frac{d}{d\xi}\left[k^*(T)\left[t_b-\delta^*\left(\frac{\xi}{L}\right)\right]\frac{dT}{d\xi}\right] = h^*(T)(T-T_a) + \sigma\,\varepsilon^*\left(T^4-T_a^4\right), \mathrm{l_d} \le \xi \le \mathrm{L}. \tag{5}$$

The HTC is given as [34]:

$$h^*(T) = h_b\left[\frac{T-T_a}{T_b-T_a}\right]^n. \tag{6}$$

By using the Chilton-Colburn analogy, the convective HTC and mass transfer coefficient are associated as [35]:

$$h^* = h_D\left(c_p\right)_f Le^{\frac{2}{3}}, \tag{7}$$

and the thermal conductivity $k^*(T)$ is related with k_a which is denoted as

$$k^*(T) = k_a[1+\kappa(T-T_a)], \tag{8}$$

where Le is the Lewis number and k_a symbolizes the thermal conductivity at T_a.

When the DES base temperature is lesser, but the DES tip temperature exceeds the humid point temperature of the atmosphere around it, the DES is said to be partially wet. The fin temperature equalizes the ambient DPT at a linear location, $\xi = l_d$, on the DES, as revealed in Fig. 1. Following that, the DES is divided into two zones: a wet portion with a DES temperature below the air DPT and a dry zone with a fin surface temperature above the air DPT. Thus, the boundary conditions for the considered cases becomes:

$$\begin{aligned} T &= T_b \text{ at } \xi = 0, \\ T &= T_d \text{ at } \xi = l_d, \\ \frac{dT}{d\xi}_{\xi=l_d^-} &= \frac{dT}{d\xi}_{\xi=l_d^+} \text{ at } \xi = l_d, \\ \frac{dT}{d\xi} &= 0 \text{ at } \xi = L. \end{aligned} \tag{9}$$

To transform Eq. (4) and Eq. (5) into dimensionless forms, the subsequent non-dimensional terms are introduced.

$$\begin{gathered} \Theta = \frac{T-T_a}{T_b-T_a}, \Theta_\mathrm{d} = \frac{T_d-T_a}{T_b-T_a},\ X = \frac{\xi}{L},\ Nc = \frac{h_b L^2}{k_a t_b},\ Nr = \frac{\sigma\varepsilon^* L^2}{k_a t_b}(T_b-T_a)^3,\ Nt = \frac{T_a}{T_b-T_a},\ L_d = \frac{l_d}{L}, \\ \beta = \kappa(T_b-T_a),\ \psi = \frac{h_b i_{fg} b_2 L^2}{\left(c_p\right)_f Le^{2/3} k_a t_b},\ \omega-\omega_a = b_2(T-T_a),\ C = \frac{\delta^*}{t_b}. \end{gathered} \tag{10}$$

The C value for dovetail profile fin is taken to be negative and the nondimensional forms of Eqs. (4) and (5) are given as:

$$\frac{d}{dX}\left[(1+\beta\,\Theta)(1-CX)\frac{d\Theta}{dX}\right] - Nc\,\Theta^{n+1} - Nr\left[(\Theta+Nt)^4 - Nt^4\right] - \psi\,\Theta^{n+1} = 0, 0 \le X \le L_d, \tag{11}$$

and

$$\frac{d}{dX}\left[(1+\beta\,\Theta)(1-CX)\frac{d\Theta}{dX}\right]-Nc\,\Theta^{n+1}-Nr\left[(\Theta+Nt)^4-Nt^4\right]=0, L_d\le X\le 1\,. \tag{12}$$

Where, *Nr* denotes the radiation-conduction parameter, *Nc* represents the convection-conduction parameter, ψ is the wet parameter, β signifies the thermal conductivity parameter, and *Nt* refer to the temperature ratio parameter. Correspondingly, Eq. (9) is reduced as:

$$\begin{aligned}\Theta&=1 \text{ at } X=0,\\ \Theta&=\Theta_d \text{ at } X=L_d,\\ \Theta^{`}|_{X=L_d^-}&=\Theta^{`}|_{X=L_d^+} \text{ at } X=L_d,\\ \Theta^{`}&=0 \text{ at } X=1.\end{aligned} \tag{13}$$

3. Neural network with Levenberg-Marquardt scheme

A neural network is a machine learning strategy influenced by biological neural networks, which replicate the neurological behavior of humans. An artificial neural network (ANN) benefits the potential to analyze large, complex data sets that are difficult to simplify using traditional statistical techniques. The fundamental building block of ANN, which can discover hidden correlations between input and output datasets, is an artificial neuron, which mimics biological neurons. As a result, ANN is frequently used to perform the desired operations via its neurons for data fitting, grouping, prediction, and other tasks. ANNs usually involve three distinct layers, which are an input layer, a hidden layer, and an output layer. The hidden layer's number of neurons can be adjusted according to the problem's complexity.

In addition, many kinds of algorithms can be used in an ANN to solve the optimization problem associated with the ANN model. Levenberg-Marquardt (LM), Bayesian Regularization, and Scaled Conjugate Gradient are such algorithms. LM algorithm is a typical optimization technique which incorporates the Gauss Newton method and the gradient descent approach. LM strategy is implemented in this investigation owing to its operational precision and capacity for accomplishing an efficient outcome in contrast to other algorithms. Utilizing statistical metrics, primarily the Mean square error (MSE) and coefficient of correlation (R^2), the effectiveness of the chosen network is evaluated. The resulting value of MSE offers the entire efficiency of fit of the network, whereas the R^2 statistic indicates the network's general functioning. The definition of the MSE and R^2 is,

$$MSE=\frac{1}{\lambda}\sum_{\zeta=1}^{\lambda}\left(\Theta_{NUM(\zeta)}-\Theta_{NNLMS(\zeta)}\right)^2. \tag{14}$$

$$R^2=1-\left[\frac{\sum_{\zeta=1}^{\lambda}\left(\Theta_{NUM(\zeta)}-\Theta_{NNLMS(\zeta)}\right)^2}{\sum_{\zeta=1}^{\lambda}\left(\Theta_{NUM(\zeta)}\right)^2}\right]. \tag{15}$$

The corresponding error between Θ_{NUM} and Θ_{NNLMS} is given as follows,

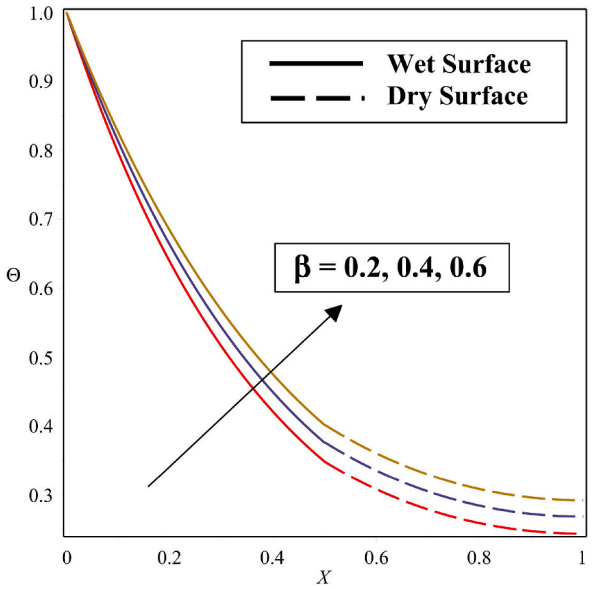

Fig. 2. Impact of β on Θ.

$$Error = \left[\frac{\Theta_{NUM(\zeta)} - \Theta_{NNLMS(\zeta)}}{\Theta_{NUM(\zeta)}}\right]. \tag{16}$$

4. Results and discussion

The impact of convective heat transmission of the dovetail fin is investigated with varying thermal conductivity and represented by the balanced heat transfer equations for partially wet and dry conditions. The balanced energy equations are non-dimensionalized using suitable dimensionless variables and numerically solved by employing RKF-45 scheme. Further, the heat transmission in a DES is studied by applying NNLMS technique. The consequence of the significant variables on temperature profile of the DES is graphically presented and are accomplished by taking particular ranges of physical parameters; $0.2 \leq \beta \leq 0.6$, $1 \leq Nc \leq 6$, $1 \leq Nr \leq 10$, $0.1 \leq Nt \leq 1$, $\psi = 0$ or 1 and $C = -0.3$. In Figs. 2–5 the impact of dry and wet conditions on the thermal profile of DES is illustrated for different parameter values. At x-axis, $X = 0.5$ is the region where the dry and wet conditions of the fin is differentiated and can be observed in respected figures. Fig. 2 portrays the thermal conductivity parameter inducement on thermal dispersion in a DES. As the values of β tends to increase (0.2, 0.4, 0.6), the fin's temperature increases. As can be detected, the mean temperature rises if the material used for the fins' thermal conductivity increases with temperature. This is due to increased quantities of the thermal conductivity parameter strengthening heat transmission through the fin, contributing to temperature rise in the DES. The upshot of the convection-conduction parameter *Nc* on the Θ of DES is displayed in Fig. 3. It is seen that the thermal distribution of DES increases as *Nc* decreases. Physically, lower material temperatures are encouraged by increased cooling efficiency due to greater convection. As increase in values of radiative-convective parameter i.e., *Nr* (1, 5, 10), decreases the thermal profile of fin as shown in Fig. 4. Radiative cooling is more efficient as the radiative transport increases, which lowers the temperatures in the fin. The fin optimally discharges heat to the adjoining environment as evidenced by the cooling temperatures within the fin when radiation strength improves. The consequence of *Nt* on temperature profile of DES is exposed in Fig. 5. Altering the scale of the ambient temperature for a fixed base temperature is the only method to upsurge the magnitude of *Nt*. From the figure, it can be seen that the Θ is decreased when scales of *Nt* (0.3, 0.5, 0.7) are increased. The aforementioned figures demonstrate that as the *X* value increases, the dimensionless temperature Θ of the DES drops gradually until it reaches a minimum temperature at the DES tip. The relative humidity is the primary factor determining whether a surface is completely wet, partially wet, or dry. When the fin is wet, the fin surface temperature typically rises as the relative humidity of the surrounding environment upsurges. This can be clarified in the context of condensation. Relative humidity increases, promoting moisture condensing on the fin surface. This improves the surface temperature by releasing more latent heat of condensation. However, when there is a relative humidity of 70%, the DPT is between the tip and base temperatures, which causes the fin to become partially wet.

The artificial neural network (ANN) model uses computing and mathematics to simulate the workings of the human brain. Many recent technological developments, such as voice and picture recognition, and robotics are related to artificial intelligence research. The ANNs structure for fins' partially wet and dry conditions is shown in Fig. 6. This ANN architecture has three layers: an input layer, a hidden layer with ten neurons, and an output unit with one neuron (as displayed in Fig. 6(a) and (b)). Each neuron has a matching design variable in the input and output layers. In this study, the ANN is trained using more accurate predictions of the thermal values at which the radiative-conductive fin must function in both partially wet and dry circumstances. The ANN's primary characteristics include splitting of the input and target dataset. The values of the non-dimensional *X* are subjected as input data and the resulting

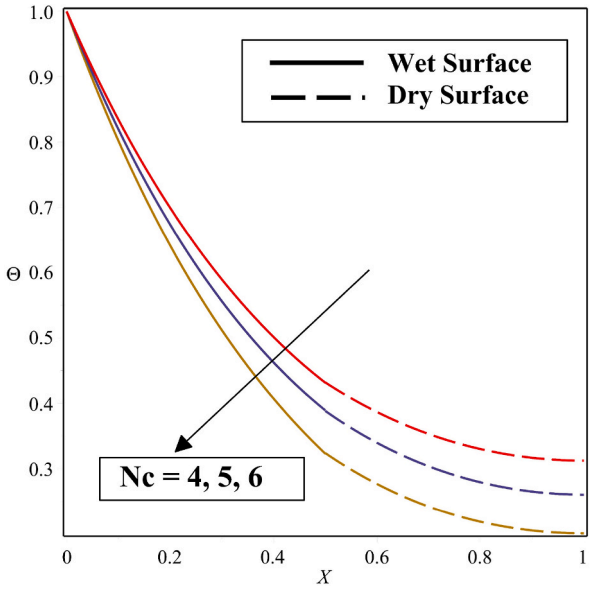

Fig. 3. Impact of *Nc* on Θ.

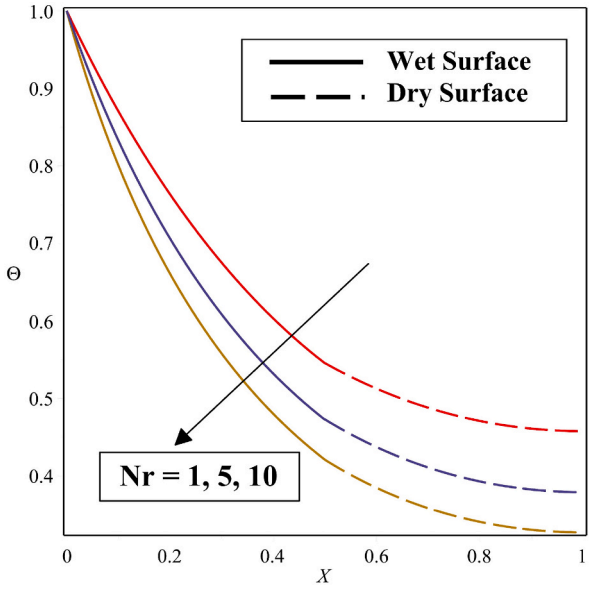

Fig. 4. Impact of *Nr* on Θ.

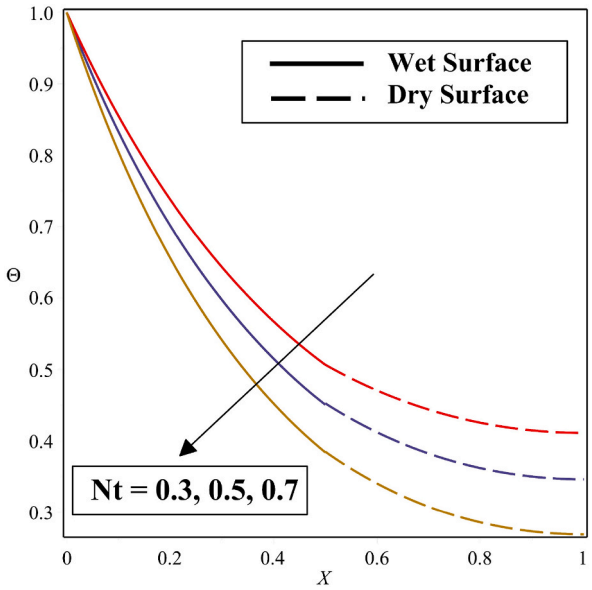

Fig. 5. Impact of *Nt* on Θ.

thermal profile values are taken as target data for the ANN training. The dataset splitting defines the group of data to be used and divides it into three parts for the construction of the ANN's training, testing, and validation phases. The datasets are structured into 70% for training, 15% for testing, and 15% for validation of the NNLMS training. Fig.s. 7(a) and 8(a) show the partially wet and partially dry conditions of the dovetail fins' validation performance as a Mean square error (MSE) indication. With an increase in epoch, the MSE level improves and performs at its best. This trained network for PWC attains its maximum value of 1.096e-11 at 315 epochs, and for partially dry conditions achieves its maximum value of 4.2482e-10 at 66 epochs. The MSE decreases as the network is trained, with epochs 315 and epochs 66 having the lowest mean square error for both conditions which can be seen in the graphs. The regression plots of the dovetail fin for partially wet and partially dry conditions are exhibited in Fig.s. 7(b) and 8(b). The figure clearly shows that the *R* is equals to one for training, testing, and validation. As a consequence, the projected behavior of the NNLMS indicated that the dovetail fin's numerical data are in good agreement with the obtained result. As an outcome, the most reliable prediction model is judged to be NNLMS. Fig.s. 7(c) and 8(c) provide the gradient, Mu, and validation values for the dovetail fins' partially wet and partially dry conditions. The resulting model shows a gradient of 9.941e-08, Mu of 1e-09, and validation of 0 at 315 epochs for

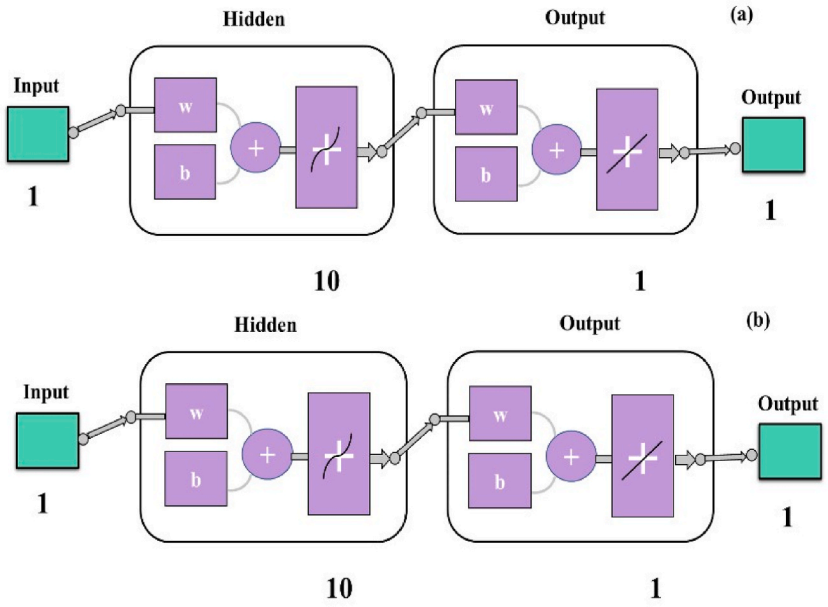

Fig. 6. Design model of NNLMS.

partially wet and gradient of 7.6542e-08, Mu of 1e-09, and validation of 0 during the 66th epoch for partially dry condition, suggesting that the network has been trained to its maximum potential. The error histogram for the partially wet and partially dry conditions of the dovetail fin are displayed in Fig.s. 7(d) and 8(d). The zero error is achieved at the value 1.98e-07 for the PWC of the dovetail fin and it is indicated as blue color line in Fig. 7(d). Similarly, for the partially dry condition, the zero error is attained at the value 6.66e-07 and it is indicated as blue color line in Fig. 8(d). The fitness plot for the partially wet and partially dry conditions of the dovetail fin is illustrated in Fig.s. 7(e) and 8(e). The training targets, training outputs, validation targets, validation outputs, test targets, and test outputs are all in good agreement for both partially wet and dry conditions of the DES.

The NNLMS solution approach and the accuracy of the accomplished findings have been validated by comparing current outcomes to the numerical results collected through the RKF-45 technique as displayed in Table 1. This table indicates that the results of NNLMS method exhibit good agreement with relatively modest errors, confirming the consistency of the NNLMS method's strategy.

5. Conclusion

The dovetail fin's thermal distribution under PWC were studied in this present work. The energy equations of the considered fin were represented in Eq. (1) and Eq. (2). The governing equations were non-dimensionalized using suitable dimensionless variables and further resulting equations were solved numerically by RKF-45 technique. NNLMS modelling was used to investigate the thermal variations of the dovetail fin for both partially wet and dry circumstances. The datasets were organized into 70% for training, 15% for testing, and 15% for validation of the NNLMS training. The repercussions of various variables on the thermal profile of a DES were graphically portrayed. These were some findings for considered fin problem:

- ❖ The thermal distribution decreased from fin's base to the dew point region of the fin under partially wetted condition and from this point, the thermal dispersal varies towards its tip.
- ❖ The temperature in a dry fin with convective heat transmission fluctuated gradually from the dew point region to the fin tip, where it equalizes with the ambient temperature.
- ❖ Relative humidity has a significant influence on the overall thermal variation of the dovetail fin for partially wet surface circumstances. Noteworthy outcomes indicated that as the thermal conductivity coefficient raised, the temperature of the dovetail extended surface elevated remarkably.
- ❖ The thermal dispersal through the fin diminished as the radiative-conductive parameter magnitude accelerated for both partially wet and dry conditions.
- ❖ An increase in convective-conductive, and temperature ratio parameter values caused to the reduction in the thermal dispersion in the dovetail fin.
- ❖ The results of the suggested NNLMS methodology demonstrated the accuracy of the method and were further supported by graphical representations of MSE convergence charts, regression, correlation analyses, and histogram investigations.
- ❖ Excellent convergence and distinctive evaluated quantified findings showed the NNLMS's effectiveness in solving the modelled nonlinear problem. Thus, the results indicated that the method had been successful in addressing the partially wetted fin problems.

The analysis discussed in this research can be expanded to examine heat transmission through various fin types in a variety of

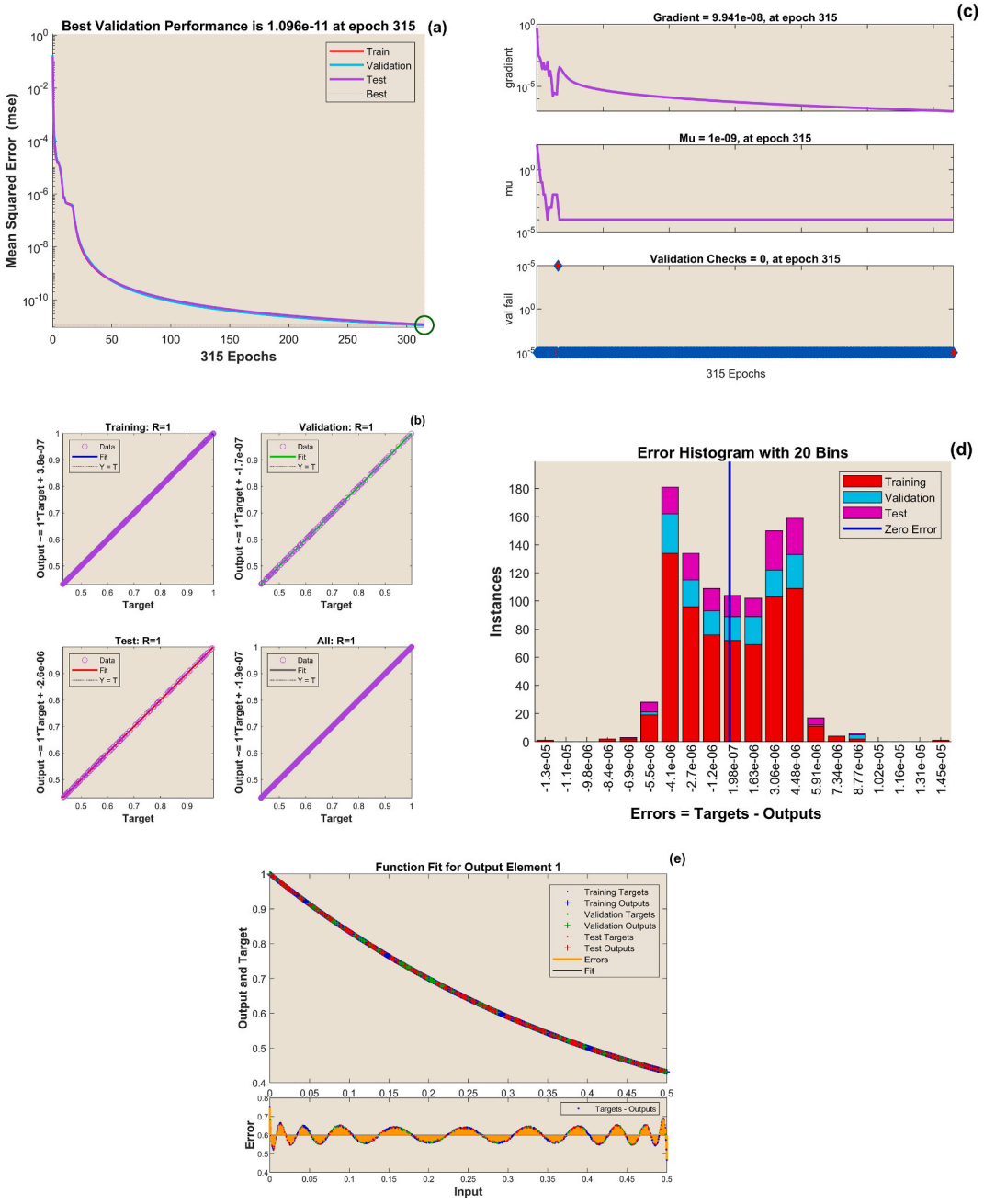

Fig. 7. Analysis of (a) Performance (b) Regression (c) Transition (d) Error histogram (e) Fitness for partially wet conditions.

conditions and physical factors. Furthermore, the presented NNLMS approach provides significant prospective results on the thermal variation in the fin. Using several types of neural networks for the fin problem, investigators can develop neural network models to achieve effective outcomes.

Author contribution statement

P. Nimmy; Pudhari Srilatha; Conceptualization, Methodology, Software, Formal analysis, Writing – original draft. K. Karthik; R. S. Varun Kumar: Writing–original draft, Resources, Data curation, Investigation, Visualization, Validation. Umair Khan; K.V. Nagaraja: Conceptualization, project administration, Funding, Writing–original draft, Writing–review & editing, Supervision, Resources. G. Sowmya: Validation, Investigation, Writing–review & editing, Formal analysis, Validation, Resources. Syed Modassir Hussain; A.S. Hendy; Mohamed R. Ali: Provided significant feedback and assisted in the revised version of the manuscript. Further, they also

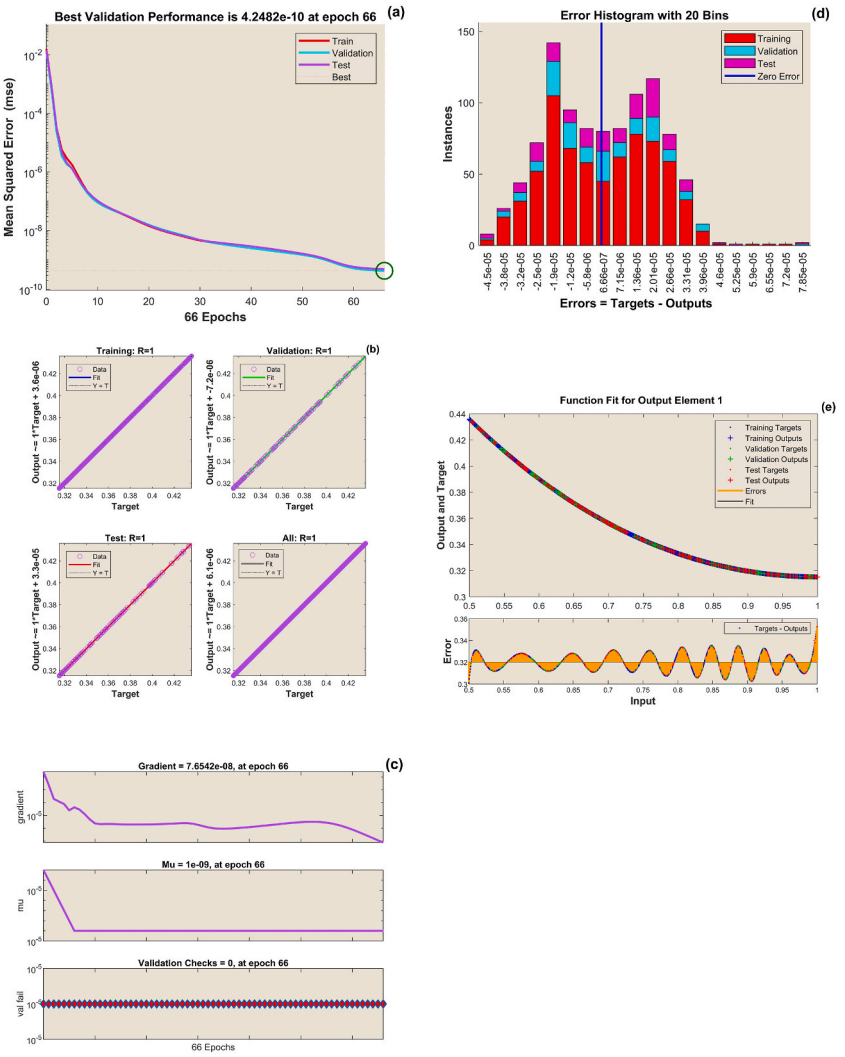

Fig. 8. Analysis of (a) Performance (b) Regression (c) Transition (d) Error histogram (e) Fitness for partially dry conditions.

Table 1
Validation of the NNLMS outcomes against RKF-45 results for partially wet and dry conditions of the DES.

X	$\Theta(X)$		
	Numerical method	NNLMS	Absolute Error
0	1	0.999984	1.52e-05
0.1	0.834396	0.834394	1.84e-06
0.3	0.589438	0.589439	1.81e-06
0.5	0.435866	0.435913	4.80e-05
0.7	0.356234	0.356214	1.98e-05
0.9	0.319584	0.319609	2.54e-05
1	0.315222	0.315140	8.17e-05

supported in revising the manuscript critically for important intellectual content.

Declaration of competing interest

It is declared that we have no conflict of interest.

Data availability

Data will be made available on request.

Acknowledgments

The researchers wish to extend their sincere gratitude to the Deanship of Scientific Research at the Islamic University of Madinah for the support provided to the Post-Publishing Program 2.

References

[1] A. Alhadhrami, C.S. Vishalakshi, B.M. Prasanna, B.R. Sreenivasa, H.A.H. Alzahrani, R.J. Punith Gowda, R. Naveen Kumar, Numerical simulation of local thermal non-equilibrium effects on the flow and heat transfer of non-Newtonian Casson fluid in a porous media, Case Stud. Therm. Eng. 28 (2021), 101483, https://doi.org/10.1016/j.csite.2021.101483.
[2] P. Sunthrayuth, S.A.M. Abdelmohsen, M.B. Rekha, K.R. Raghunatha, A.M.M. Abdelbacki, M.R. Gorji, B.C. Prasannakumara, Impact of nanoparticle aggregation on heat transfer phenomena of second grade nanofluid flow over melting surface subject to homogeneous-heterogeneous reactions, Case Stud. Therm. Eng. 32 (2022), 101897, https://doi.org/10.1016/j.csite.2022.101897.
[3] K. Rafique, Z. Mahmood, U. Khan, Mathematical analysis of MHD hybrid nanofluid flow with variable viscosity and slip conditions over a stretching surface, Mater. Today Commun. 36 (2023), 106692, https://doi.org/10.1016/j.mtcomm.2023.106692.
[4] Z. Mahmood, M.A. El-Rahman, U. Khan, A.M. Hassan, H.A.E.-W. Khalifa, Entropy generation due to nanofluid flow in porous media over radiative permeable exponentially surface with nanoparticle aggregation effect, Tribol. Int. 188 (2023), 108852, https://doi.org/10.1016/j.triboint.2023.108852.
[5] M. Nagapavani, G.V. Ramana Reddy, A. Abdulrahman, R. Kumar, R.J. Punith Gowda, Three-dimensional swirling flow of a ternary composite nanofluid induced by the torsional motion of a cylinder considering non-Fourier law, Numer. Heat Tran., Part A: Applications (2023) 1–14, https://doi.org/10.1080/10407782.2023.2219834, 0.
[6] K. Rafique, Z. Mahmood, U. Khan, S.M. Eldin, M. Oreijah, K. Guedri, H.A.E.-W. Khalifa, Investigation of thermal stratification with velocity slip and variable viscosity on MHD flow of Al2O3−Cu−TiO2/H2O nanofluid over disk, Case Stud. Therm. Eng. 49 (2023), 103292, https://doi.org/10.1016/j.csite.2023.103292.
[7] P. Srilatha, H. Abu-Zinadah, R.S.V. Kumar, M.D. Alsulami, R.N. Kumar, A. Abdulrahman, R.J. Punith Gowda, Effect of nanoparticle diameter in maxwell nanofluid flow with thermophoretic particle deposition, Mathematics 11 (2023) 3501, https://doi.org/10.3390/math11163501.
[8] K. Rafique, Z. Mahmood, A.M. Alqahtani, A.M.A. Elsiddieg, U. Khan, W. Deebani, M. Shutaywi, Impacts of thermal radiation with nanoparticle aggregation and variable viscosity on unsteady bidirectional rotating stagnation point flow of nanofluid, Mater. Today Commun. 36 (2023), 106735, https://doi.org/10.1016/j.mtcomm.2023.106735.
[9] A.H. Ganie, Z. Mahmood, M.M. AlBaidani, N.S. Alharthi, U. Khan, Unsteady non-axisymmetric MHD Homann stagnation point flow of CNTs-suspended nanofluid over convective surface with radiation using Yamada–Ota model, Int. J. Mod. Phys. B (2023), 2350320, https://doi.org/10.1142/S0217979223503204.
[10] P.L. Ndlovu, The significance of fin profile and convective-radiative fin tip on temperature distribution in a longitudinal fin, Nano Hybrids and Composites 26 (2019) 93–105. https://doi.org/10.4028/www.scientific.net/NHC.26.93.
[11] D. Umrao Sarwe, V.S. Kulkarni, Differential transformation method to determine heat transfer in annular fins, Heat Transfer 50 (2021) 7949–7971, https://doi.org/10.1002/htj.22261.
[12] Z.U. Din, A. Ali, S. Ullah, G. Zaman, K. Shah, N. Mlaiki, Investigation of heat transfer from convective and radiative stretching/shrinking rectangular fins, Math. Probl Eng. (2022), e1026698, https://doi.org/10.1155/2022/1026698, 2022.
[13] S. Gouran, S.E. Ghasemi, S. Mohsenian, Effect of internal heat source and non-independent thermal properties on a convective–radiative longitudinal fin, Alex. Eng. J. 61 (2022) 8545–8554, https://doi.org/10.1016/j.aej.2022.01.063.
[14] R.S.V. Kumar, I.E. Sarris, G. Sowmya, A. Abdulrahman, Iterative solutions for the nonlinear heat transfer equation of a convective-radiative annular fin with power law temperature-dependent thermal properties, Symmetry 15 (2023) 1204, https://doi.org/10.3390/sym15061204.
[15] N. Acharya, Buoyancy driven magnetohydrodynamic hybrid nanofluid flow within a circular enclosure fitted with fins, Int. Commun. Heat Mass Tran. 133 (2022), 105980, https://doi.org/10.1016/j.icheatmasstransfer.2022.105980.
[16] I. Waini, U. Khan, A. Zaib, A. Ishak, I. Pop, Inspection of TiO2-CoFe2O4 nanoparticles on MHD flow toward a shrinking cylinder with radiative heat transfer, J. Mol. Liq. 361 (2022), 119615, https://doi.org/10.1016/j.molliq.2022.119615.
[17] N. Acharya, A.J. Chamkha, On the magnetohydrodynamic Al2O3-water nanofluid flow through parallel fins enclosed inside a partially heated hexagonal cavity, Int. Commun. Heat Mass Tran. 132 (2022), 105885, https://doi.org/10.1016/j.icheatmasstransfer.2022.105885.
[18] N. Acharya, On the magnetohydrodynamic natural convective alumina nanofluidic transport inside a triangular enclosure fitted with fins, J. Indian Chem. Soc. 99 (2022), 100784, https://doi.org/10.1016/j.jics.2022.100784.
[19] H.J. Lane, P.J. Heggs, Extended surface heat transfer—the dovetail fin, Appl. Therm. Eng. 25 (2005) 2555–2565, https://doi.org/10.1016/j.applthermaleng.2004.11.031.
[20] N.A. Khan, M. Sulaiman, F.S. Alshammari, Heat transfer analysis of an inclined longitudinal porous fin of trapezoidal, rectangular and dovetail profiles using cascade neural networks, Struct. Multidiscip. Optim. 65 (2022) 251, https://doi.org/10.1007/s00158-022-03350-6.
[21] F. Gamaoun, A. Abdulrahman, G. Sowmya, R. Kumar, U. Khan, A.M. Alotaibi, S.M. Eldin, R.S. Varun Kumar, Non-Fourier heat transfer in a moving longitudinal radiative-convective dovetail fin, Case Stud. Therm. Eng. 41 (2023), 102623, https://doi.org/10.1016/j.csite.2022.102623.
[22] J.F. Mao, B. Wang, S.B. Geng, L.Y. Sui, 2-D numerical analysis of fin efficiency on straight rectangular fin with combined heat and mass transfer, Appl. Mech. Mater. 105–107 (2012) 2117–2120. https://doi.org/10.4028/www.scientific.net/AMM.105-107.2117.
[23] W. Pirompugd, S. Wongwises, Partially wet fin efficiency for the longitudinal fins of rectangular, triangular, concave parabolic, and convex parabolic profiles, J. Franklin Inst. 350 (2013) 1424–1442, https://doi.org/10.1016/j.jfranklin.2013.02.019.
[24] S. Pashah, A. Moinuddin, S.M. Zubair, Thermal performance and optimization of hyperbolic annular fins under dehumidifying operating conditions – analytical and numerical solutions, Int. J. Refrig. 65 (2016) 42–54, https://doi.org/10.1016/j.ijrefrig.2016.01.006.
[25] S.A. Hazarika, D. Bhanja, S. Nath, Fork-shaped constructal fin array design a better alternative for heat and mass transfer augmentation under dry, partially wet and fully wet conditions, Int. J. Therm. Sci. 152 (2020), 106329, https://doi.org/10.1016/j.ijthermalsci.2020.106329.
[26] W. Pirompugd, S. Wongwises, Analytical methods for the efficiency of annular fins with rectangular and hyperbolic profiles under partially wet surface conditions, Numer. Heat Tran., Part A: Applications 80 (2021) 617–634, https://doi.org/10.1080/10407782.2021.1969175.
[27] H. Pothina, K.V. Nagaraja, Artificial neural network and math behind it, in: Y.-D. Zhang, T. Senjyu, C. So-In, A. Joshi (Eds.), Smart Trends in Computing and Communications, Springer Nature, Singapore, 2023, pp. 205–221, https://doi.org/10.1007/978-981-16-9967-2_21.
[28] P. Naphon, S. Wiriyasart, T. Arisariyawong, L. Nakharintr, ANN, numerical and experimental analysis on the jet impingement nanofluids flow and heat transfer characteristics in the micro-channel heat sink, Int. J. Heat Mass Tran. 131 (2019) 329–340, https://doi.org/10.1016/j.ijheatmasstransfer.2018.11.073.
[29] I. Ahmad, H. Zahid, F. Ahmad, M.A.Z. Raja, D. Baleanu, Design of computational intelligent procedure for thermal analysis of porous fin model, Chin. J. Phys. 59 (2019) 641–655, https://doi.org/10.1016/j.cjph.2019.04.015.
[30] A.N. Skrypnik, A.V. Shchelchkov, YuF. Gortyshov, I.A. Popov, Artificial neural networks application on friction factor and heat transfer coefficients prediction in tubes with inner helical-finning, Appl. Therm. Eng. 206 (2022), 118049, https://doi.org/10.1016/j.applthermaleng.2022.118049.

[31] R.S. Varun Kumar, I.E. Sarris, G. Sowmya, B.C. Prasannakumara, A. Verma, Artificial neural network modeling for predicting the transient thermal distribution in a stretching/shrinking longitudinal fin, ASME J.Heat and Mass Transfer 145 (2023), https://doi.org/10.1115/1.4062215.

[32] C. Kumar, P. Nimmy, K.V. Nagaraja, R.S.V. Kumar, A. Verma, S. Alkarni, N.A. Shah, Analysis of heat transfer behavior of porous wavy fin with radiation and convection by using a machine learning technique, Symmetry 15 (2023) 1601, https://doi.org/10.3390/sym15081601.

[33] B. Kundu, Approximate analytic solution for performances of wet fins with a polynomial relationship between humidity ratio and temperature, Int. J. Therm. Sci. 48 (2009) 2108–2118, https://doi.org/10.1016/j.ijthermalsci.2009.03.005.

[34] J. Suresh Goud, P. Srilatha, R.S. Varun Kumar, G. Sowmya, F. Gamaoun, K.V. Nagaraja, J. Singh Chohan, U. Khan, S.M. Eldin, Heat transfer analysis in a longitudinal porous trapezoidal fin by non-Fourier heat conduction model: an application of artificial neural network with Levenberg–Marquardt approach, Case Stud. Therm. Eng. 49 (2023), 103265, https://doi.org/10.1016/j.csite.2023.103265.

[35] A. Abdulrahman, F. Gamaoun, R.S. Varun Kumar, U. Khan, H. Singh Gill, K.V. Nagaraja, S.M. Eldin, A.M. Galal, Study of thermal variation in a longitudinal exponential porous fin wetted with TiO2−SiO2/hexanol hybrid nanofluid using hybrid residual power series method, Case Stud. Therm. Eng. 43 (2023), 102777, https://doi.org/10.1016/j.csite.2023.102777.